Journal of Petroleum Science and Engineering 136 (2015) 23–31

Contents lists available at ScienceDirect

Journal of Petroleum Science and Engineering

journal homepage: www.elsevier.com/locate/petrol

Inflow performance of wells intersecting long fractures with transient pressure and variable flow-rate behavior

R.O. Vargas [a,*], C. Lira-Galeana [b], D. Silva [c], O. Manero [d]

[a] ESIME Azcapotzalco, Instituto Politécnico Nacional, Av. de las Granjas 682, Col. Santa Catarina, Del. Azcapotazalco, México, D.F. 02250, Mexico
[b] Instituto Méxicano del Petróleo, Eje Central Lázaro Cárdenas Norte 152, San Bartolo Atepehuacan, México, D.F. 07730, Mexico
[c] Universidad de Guanajuato, División de Ingenierías Sede San Matías, Ex-Hacienda de San Matías s/n, Col. San Javier, Guanajuato, Gto., México CP 36020, Mexico
[d] Instituto de Investigaciones en Materiales, Universidad Nacional Autónoma de México (UNAM), Ciudad Universitaria, México, D.F. CP 04510, Mexico

ARTICLE INFO

Article history:
Received 2 June 2014
Received in revised form
25 September 2015
Accepted 31 October 2015
Available online 2 November 2015

Keywords:
Mathematical model
Oil wells
Hydraulically induced fractures
Transient pressure and flow rate

ABSTRACT

A mathematical model which predicts the performance of vertical and horizontal wells intersecting fractures is presented. Based on the formulation originally proposed by Guo and Schechter (1997), this model predicts the transient pressure behavior with variable flow-rate both during the increasing pressure stage and in the declining pressure and flow-rate situation. The flow in the matrix and that in the fracture are coupled to allow the calculation of the pressure distribution in the matrix and in the fracture, as functions of space and time. The model is consistent with transient pressure analyses in finite-conductivity vertical fractures (Cinco-Ley and Samaniego, 1981), and presents a useful tool for productivity analyses of hydraulically fractured wells during the rapid decline stage. Comparisons with real well data are analyzed and discussed.

1. Introduction

Several factors control the final output of the hydraulic fracturing process. Fracture dimensions (half fracture length, fracture width, and fracture height) are of particular importance together with data related to the orientation of fractures as well as the rock and fluid properties (Rbeawi and Tiab, 2012). The Naturally Fractured Reservoirs (NFR) are among the most common and important reservoirs around the world, due to the large extent of oil reserves therein contained. The NFR have a very complex structure and therefore, mathematical models which may predict the pressure behavior are needed. These models are classified according to the inter-porosity transfer flow regime and they are based on Warren and Root's theory (Cinco-Ley and Samaniego, 1981; Najurieta, 1980; Ley and Samaniego, 1982; Streltsova, 1982).

Nelson (1985) categorized naturally fractured reservoirs into four different types, with regard to reservoir simulations and performance, and pressure and rate-transient-test interpretation. Kuchuk and Biryukov (2012), on the other hand, divide them into four categories: (a) continuously (dual-porosity) fractured reservoirs, (b) discretely fractured reservoirs, (c) compartmentalized faulted basement reservoirs and (d) unconventional fractured basement reservoirs. Biryukov and Kuchuk (2012) and Kuchuk and Biryukov (2012) presented transient-pressure solutions for conductive and nonconductive faults and fractures, and showed their pressure-transient behavior. Kuchuk and Biryukov (2012) investigated the pressure transient behavior of continuous and discrete naturally fractured reservoir with semianalytical solutions for a vertical well, they performed history matching of the pressure-transient data generated from their discrete and continuously fractured reservoir models with the Warren and Root (1963) dual porosity type models obtaining incorrect reservoir parameters.

Attention has been focused on the modeling of the pressure transient behavior for either horizontal or vertical wells, with or without hydraulic fractures. As a result, several models were developed based on the use of the source solution and Green's function to solve unsteady-state flow problems in the reservoir. Gringarten and Ramey (1973) used the source function and Newman product method for solving transient flow problem. Although this approach is extremely powerful in solving 2D and 3D problems, it has some limitations related to incorporate the influence of storage and skin effects. In this context, the transient-flow solutions have been extended to predict the behavior of infinite-conductivity vertical fractures in homogeneous formations or in dual-porosity media. Ozkan (1988) presented an extensive

* Corresponding author.
E-mail addresses: rvargasa@ipn.mx (R.O. Vargas), clira@imp.mx (C. Lira-Galeana), telamoniada@hotmail.com (D. Silva), manero@unam.mx (O. Manero).

http://dx.doi.org/10.1016/j.petrol.2015.10.040
0920-4105/

literature of different solutions for the diffusivity equation in terms of the Laplace transform to reduce the limitations in the source solution presented by Gringarten and Ramey (1973). Benjamin (1978) used a finite element model to study the pressure behavior of a well intersecting vertical fracture at the center of closed square reservoir. Wong et al. (1986) analyzed the data using curve-matching and pressure and its derivative for vertical-fractured wells with no skin and no wellbore storage effects, and included cases where both skin and wellbore storage effects are present during the bi-linear flow period. Cinco-Ley and Meng (1988) analyzed results obtained from the transient behavior of a well intersected by a vertical fracture in a double porosity reservoir. Two models were introduced: the first one is semi-analytical and the second one is a simplified fully-analytical model. Song et al. (2011) studied pressure transient behavior of a horizontal well with transverse fractures and provided a description of pressure transient flow regimes with corresponding analytical solutions. Raghavan et al. (1997) developed a mathematical model to discern the characteristic response of multiply fractured horizontal wells. Three significant flow periods have been observed based on this model: the early-time period in which the system behaves like one with n-layers, the intermediate-time period in which the system reflects the interference between the fractures, and late-time period in which the system behaves as a single-fracture horizontal well with equal distances between the outermost fractures. Wan and Aziz (1999) developed a general solution for horizontal wells with multiple fractures. They showed that four flow-regimes can be observed: the early-linear, transient, late-linear, and late- time radial flow. Zerzar et al. (2003) combined the boundary element method and Laplace transformation to present a comprehensive solution for multiple vertical-fractured horizontal wells. Seven flow regimes have been identified: bilinear, first-linear, elliptical, radial, pseudo-radial, second-linear, and pseudo-steady state. Al-Kobaisi and Ozkan (2004) presented a hybrid numerical–analytical model for the pressure transient response of horizontal wells intercepted by a vertical fracture. This model can be used as a pressure-transient analysis or as a diagnostic tool to interpret complex characteristics and to investigate the influence of various fracture properties on the production performance of fractured horizontal wells. Anh and Tiab(2009) solved the analytical model presented by Cinco-Ley (1974) for the pressure transient behavior caused by an inclined fracture associated to a vertical wellbore. This model uses the uniform-flux and infinite-conductivity fracture solution for different inclination angles. Both type-curve and Tiab's direct synthesis (TDS) techniques have been used to estimate formation parameters such as the permeability, skin factor, and fracture length (Boussila and Tiab, 2003). Al-Kobaisi et al. (2006) focused on the pressure-transient characteristics in the early-time flow regimes. They described the fracture-storage induced by flow regimes in multiple-transverse fractured horizontal wells.

Detailed reservoir information is essential for the petroleum engineer to analyze the current behavior and future performance of the reservoir. Pressure transient testing is designed to provide the engineer with a quantitative analysis of the reservoir properties. A transient test is essentially conducted by creating a pressure disturbance in the reservoir and recording the pressure response of the wellbore. The type-curve analysis approach was introduced in the petroleum industry by Agarwal et al. (1970). It is known that a type-curve is a graphical representation of theoretical solutions to transient and pseudo-steady-state flow equations; they are usually presented in terms of dimensionless pressure, time, wellbore radius and wellbore storage factor (e.g., P_D, t_D, r_D and C_D). The Gringarten type-curve analysis (Gringarten et al. (1970)) and the pressure-derivative method use the concept of the type-curve approach.

In this work, consideration is given to the analytical Guo and Schechter (1997) model, extended to the case of transient flow behavior. A fractal matrix and time-dependent pressure and flow variables are considered in the calculations, giving rise to matrix and fracture pressure distributions as functions of space and time in the increasing and decreasing pressure and flow-rate stages. This model can be used as a pressure-transient analysis or diagnostic tool to interpret complex characteristics and to investigate the influence of various fracture properties on the production performance of fractured horizontal wells.

2. Mathematical model

2.1. Model description

In the Guo and Schechter (1997) model, the geometry of a reservoir section drained by a fracture wing is shown in Fig. 1. We follow the development of the model allowing oil to flow within the drainage boundaries ($z = \pm ze$) to the fracture face in the z-direction. The velocity of the oil in the matrix is described by Darcy's law:

$$v_z(x) = \frac{k_m}{\mu z_e}(p_e - p_f(x)), \tag{1}$$

where $v_z(x)$ is the Darcy velocity in the z-direction within the matrix at a lateral distance x from the fracture tip. μ is the oil viscosity, z_e is the drainage distance of the fracture, p_e is the pressure at the drainage boundary, $p_f(x)$ is the pressure in the fracture at point x and k_m is the matrix permeability. It has been shown that the porosity and fractures of geological formations exhibit fractal characteristics under many length scales (Katz and Thompson, 1985), and that the nature of the fractal porous medium influences their transport properties (Schmittbuhl et al., 2008). Makse et al. (2000) found that the permeability of porous media decreases when the fractal dimension (associated to pores space) decreases. In this model, the flow into the fracture through the porous matrix along the z-axis is considered, since the pores are interconnected to form channels or capillaries. The permeability in the porous or fractal medium can be evaluated following Turcio et al. (2013):

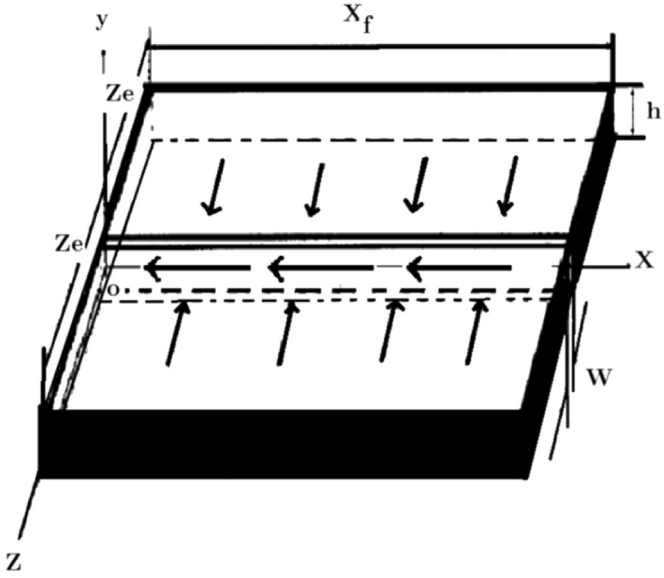

Fig. 1. Geometry of a reservoir section drained by a wing of a fracture. The wellbore is located at $x = y = z = 0$. Oil flows along the z-direction.

$$k_m = \frac{2^{2D_T-2}\phi(3-D_T-D_f)}{8D_T L_0^{2D_T-2}}\left[1-\left(\frac{r_{min}}{r_{max}}\right)^{3-D_T-D_f}\right]^{-1}. \quad (2)$$

Here k_m is the function of the porosity ϕ, the characteristic length L_0, the minimum and maximum porous radii (r_{min} and r_{max}) and the fractal dimensions D_T and D_f. The volumetric flow rate of oil in the fracture at point x can be determined by:

$$Q(x) = 2h\int_0^x v_z(x)\,dx = \frac{2hk_m}{\mu z_e}\int_0^x [p_e - p_f(x)]\,dx, \quad (3)$$

where $Q(x)$ is the volumetric flow rate in the fracture at point x and h is the fracture height. If the average width of the fracture is w, the velocity in the fracture $v_f(x)$ can be calculated:

$$v_f(x) = \frac{Q(x)}{hw} = \frac{-2k_m}{k_f w z_e}\int_0^x [p_e - p_f(x)]\,dx. \quad (4)$$

The Darcy velocity in the fracture with permeability k_f is:

$$v_f(x) = -\frac{k_f}{\mu}\frac{d}{dx}p_f(x), \quad (5)$$

substituting Eq. (4) into Eq. (5) yields:

$$\frac{d}{dx}p_f(x) = \frac{-2k_m}{k_f w z_e}[p_e - p_f(x)]\,dx, \quad (6)$$

differentiation of Eq. (6) with respect to x gives:

$$\frac{d^2}{dx^2}p_f(x) = \frac{-2k_m}{k_f w z_e}[p_e - p_f(x)], \quad (7)$$

Eq. (7) may be rewritten in the following form:

$$\frac{d^2}{dx^2}p_f(x) + \frac{2}{F_{CD}z_e x_j}[p_e - p_f(x)] = 0, \quad (8)$$

where F_{CD} is the dimensionless conductivity in the fracture

$$F_{CD} = \frac{k_f w}{k_m x_f}. \quad (9)$$

Eq. (8) is the same equation used by Cinco-Ley and Samaniego (1981) in steady-state, i.e.,

$$\frac{1}{\eta_{fD}}\frac{\partial p_{fD}}{\partial t_f} = \frac{\partial^2 p_f(x)}{\partial x_D^2} + \frac{2}{F_{CD}}\frac{\partial p_D}{\partial z_D}\bigg|_{z_d=0} = 0, \quad (10)$$

where the pressure gradient of the fracture-matrix interface is:

$$\frac{\partial p_D}{\partial z_D} = \frac{p_e - p_f(x)}{z_e}. \quad (11)$$

The z-coordinate is equivalent to the y-coordinate in the Cinco-Ley and Samaniego (1981) reference system. The boundary conditions for Eq. (8) are:

$$\text{At } x = 0 \quad p_f(x) = p_w \quad \text{(in the wellbore)}, \quad (12)$$

$$\frac{d}{dx}p_f(x) = 0, \quad p_f = p_e \ (v_f = 0 \text{ at the edge of the fracture}). \quad (13)$$

The second condition was also considered by Cinco-Ley and Samaniego (1981) for the infinite well case. The analytical solution of Eq. (8) subjected to boundary conditions given in Eqs. (12) and (13) is

$$p_e - p_f(x) = [p_e - p_w]\exp(-\sqrt{cx}), \quad (14)$$

where $c = 2/(FCDz_e x_f)$. Note that the pressure in the fracture p_f varies from p_w at the wellbore ($x=0$) and the difference $(p_e - p_f)$ decreases exponentially. p_e is only attained when c has a large value (very small conductivity ratio). If the conductivity ratio is large, c is very small and hence the steady-state pressure in the fracture is near p_w. The volumetric flow-rate in the fracture can be evaluated using Eq. (3). Substituting Eq. (14) into Eq. (3) we obtain:

$$Q = \frac{2hk_m}{\mu z_e}\int_0^{x_f}[p_e - p_f(x)]\,dx = \frac{2hk_m}{\mu\sqrt{cz_e}}(p_e - p_w)(1-\exp(-\sqrt{c(x_f)})). \quad (15)$$

Note that when the fracture length is large, the flow rate is proportional to the pressure gradient between wellbore and that at the edge of the matrix. The pressure distribution in the matrix $p_m(x, z)$ can be obtained analytically considering linear flow:

$$P^* = \frac{p_m - p_f(x)}{p_e - p_f(x)} = \frac{z}{z_e} = z^*. \quad (16)$$

Upon substitution of Eq. (14) into Eq. (16), the following expression is obtained:

$$p_m - p_f(x) = z^*[p_e - p_w]\exp(-\sqrt{cx}). \quad (17)$$

2.2. Transient regime

The solution of the pressure diffusion equation along the fracture (Eq. (10)) requires the solution of the time-dependent problem of the matrix, which is expressed by the following pressure-diffusion equation:

$$\frac{\partial p_m}{\partial t^*} = \frac{\partial^2 p_m}{\partial z^{*2}}, \quad (18)$$

where $t^* = t\eta_m$ is the dimensionless time and η_m is the matrix hydraulic diffusivity. Eq. (16) is the solution of Eq. (18) at large times. Thereafter, it is necessary to evaluate the pressure gradient in the matrix at the interface $(dpm/dz^*)_{z=0}$, and finally solving the time-dependent Eq. (10). Solution of Eq. (18) is:

$$p^* = \frac{p_m(x, z^*, t^*) - p_f(x)}{p_e - p_f(x)} = z^* + \frac{2}{\pi}\sum_{n=1}^{\infty}\frac{(-1^n)}{n}\sin(n\pi z^*)\exp(-n^2\pi^2 t^*). \quad (19)$$

This equation satisfies the initial condition:

$$t = 0 \quad p_m(x, z^*, t^*) = p_f(x') \quad \text{or} \quad p^* = 0, \quad (20)$$

since the following equality holds: $\frac{2}{\pi}\sum_{n=1}^{\infty}\frac{(-1)^n}{n}\sin(n\pi z^*) = -z^*$, as $t \to \infty$ the steady-state solution is attained, i.e., $p^* = z^*$. This condition implies that the initial pressure distribution in the matrix follows the pressure distribution along the interface with the fracture (linear flow in the fracture).

Boundary conditions for Eq. (18) are:

$$z^* = 0, \quad p_m = p_f(x) \text{ at the interface} \quad (p^* = 0), \quad (21)$$

$$z^* = 1, \quad p_m = p_e(x) \text{ at the far edge of the matrix} \quad (p^* = 1). \quad (22)$$

The matrix pressure gradient along the interface $(dpm/dz^*)_{z=0}$ can be calculated using Eq. (19):

$$\frac{1}{p_e - p_f(x)} = 1 + 2\sum_{n=1}^{\infty}(-1)^n\cos(n\pi z^*)\exp(-n^2\pi^2 t^*), \quad (23)$$

at the fracture-formation interface:

$$\frac{1}{p_e - p_f(x)}\left|\frac{dp_m}{dz^*}\right|_{z^*=0} = 1 + 2\sum_{n=1}^{\infty}(-1)^n \exp(-n^2\pi^2 t^*). \tag{24}$$

Substituting Eq. (24) into Eq. (10), the time-dependent equation for the pressure in the fracture to solve is:

$$\frac{1}{\eta_f}\frac{\partial^2 p_f}{\partial x^2} + \frac{2}{F_{CD}}\frac{1}{z_e}(p_e - p_f)(1 + 2\sum_{n=1}^{\infty}(-1)^n \exp(-n^2\pi^2 t^*)), \tag{25}$$

where η_f is now the fracture diffusivity with the initial condition given by Eq. (20) and with boundary conditions:

$$\text{At } x = 0, \quad p_w = p_f(x), \tag{26}$$

$$\text{At } x = x_f, \quad p_e = p_f(x). \tag{27}$$

2.3. Flow rate

The time-dependent oil flow rate can be evaluated as follows:

$$Q = \frac{2hk_m}{\mu z_e}\int_0^{x_f}\left|\frac{\partial p_m}{\partial z^*}\right| dx \tag{28}$$

Substituting Eq. (14) into Eq. (24) yields:

$$\left|\frac{dp_m}{dz^*}\right|_{z^*=0} = (p_e - p_w)\exp(-\sqrt{cx})(1 + 2\sum_{n=1}^{\infty}(-1)^n \exp(-n^2\pi^2 t^*)), \tag{29}$$

substitution of Eq. (29) into Eq. (28) and upon integration:

$$Q = \frac{2hk_m}{\mu\sqrt{c}z_e}(p_e - p_w)(1 - \exp(-\sqrt{c(x_f)}))(1 - f(t)), \tag{30}$$

where the time-dependent function $f(t)$ has the form:

$$f(t) = 2\sum_{n=1}^{\infty}(-1)^n \exp(-n^2\pi^2 t^*). \tag{31}$$

Initially, at $t=0$, $Q=0$, since due to Fejer's theorem,

$$2\sum_{n=1}^{\infty}(-1)^n = -1, \tag{32}$$

for large times, $f(t) = 0$, the flow rate reaches the maximum value at steady-state (see Eq. (38)). The asymptotic solution of Eq. (38) at large times for the case when the fracture conductivity is also large $(c \to 0)$ is:

$$Q = \frac{2hk_m}{\mu z_e}(p_e - p_w)(x_f). \tag{33}$$

This equation represents the maximum attainable flow-rate. For higher values of c (decreasing fracture conductivity) a decrease of the flow rate for long times is expected.

2.4. Declining pressure and flow-rate regimes

To model this behavior, a change in the boundary conditions in Eq. (18) is made. Initially, the pressure and flow rate are at their maxima, and for subsequent times, p^* and Q tend asymptotically to zero. Therefore, the solution equation (19) is modified to:

$$p^* = z^* + \frac{2}{\pi}\sum_{n=1}^{\infty}(-1)^n(1 - \exp(-n^2\pi^2 t^*)). \tag{34}$$

Initially, at time zero the steady-state solution is confirmed, i.e., $p^* = z^*$. For long times, Eq. (34) tends to $p^* = 0$. Calculation of the pressure gradient gives:

$$\frac{1}{p_e - p_f(x')}\frac{dp_m}{dz^*} = 1 + 2\sum_{n=1}^{\infty}(-1)^n(1 - \exp(-n^2\pi^2 t^*), \tag{35}$$

at the interface:

$$\frac{1}{p_e - p_f(x')}\left|\frac{dp_m}{dz^*}\right|_{z^*=0} = 1 + 2\sum_{n=1}^{\infty}(-1)^n(1 - \exp(-n^2\pi^2 t^*)), \tag{36}$$

substituting Eq. (36) into Eq. (28) gives:

$$Q = \frac{2hk_m}{\mu\sqrt{c}z_e}(p_e - p_w)(1 - e^{-\sqrt{c(x_f)}})\,(1 + 2\sum_{n=1}^{\infty}(-1)^n(1 - \exp(-n^2\pi^2 t^*))), \tag{37}$$

at short times, we obtain Eq. (38) for the flow rate:

$$Q = \frac{2hk_m}{\mu\sqrt{cz_e}}(p_e - p_w)(1 - \exp(-\sqrt{c(x_f)})). \tag{38}$$

For long times, the pressure gradient at the interface tends to zero, and hence the flow rate.

3. Results and discussion

In this section, the analytical and numerical predictions of the model are presented. Fig. 2 presents the pressure along the fracture length for various conductivity ratios (Eq. (14)). The pressure increases from its value at the wellbore, up to the maximum pressure (reservoir pressure or drainage pressure), but depends strongly on the conductivity ratio. Lower c-values correspond to larger fracture conductivities. For large fracture conductivity, the pressure increases from the wellbore pressure $(x = 0)$ up to the reservoir pressure along a large distance. For decreasing fracture conductivity, the reservoir pressure is attained in short distance from the wellbore. Hence, the effective pressure gradient along the fracture increases as the conductivity in the fracture diminishes. This behavior is the same presented by Guo and Schechter (1997) at steady-state. Fig. 3 presents results according to Eq. (38), where the flow rate is plotted with permeability ratio. As the permeability in the fracture increases, the flow rate increases exponentially. With respect to the matrix pressure distribution,

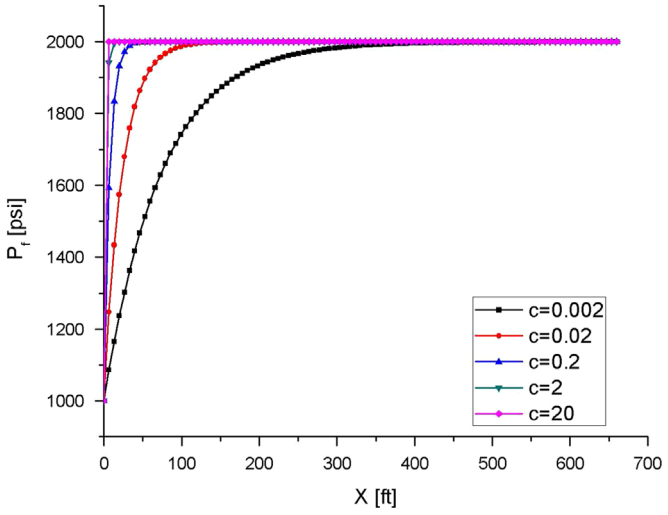

Fig. 2. Pressure along the fracture length as a function length for various fracture conductivities. w=0.001 m, x_f = 200 m, z_e = 200 m, p_e = 2000 psi, p_w = 1000 psi.

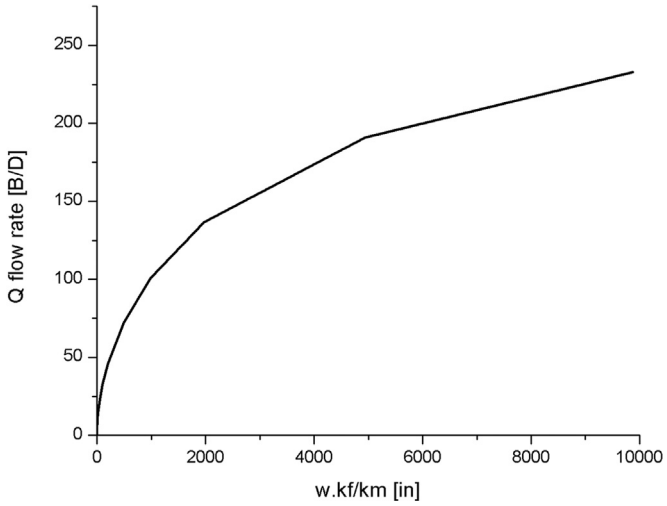

Fig. 3. Flow rate as a function of permeability ratio.

Fig. 4a–d depicts the steady-state or long-time isobaric profiles in the z–x plane for various permeability ratios. The wellbore is located at the origin $(z = 0, x = 0)$, the fracture is located at $(z = 0, 0 < x < 1)$ and the edge of the reservoir length is $z=1$ for $0 < x < 1$. There are two fixed pressures: the reservoir pressure pe and the wellbore pressure pw; the reservoir pressure is fixed at $(z = 1, 0 < x < 1)$. The maximum pressure gradient $(p_e - p_w)/z_e$ in highly conductive fractures covers a good proportion of the fracture length, since the pressure in the fracture approaches the pressure in the wellbore. As the conductivity ratio diminishes (Fig. 4d) there are progressively smaller fracture lengths where the pressure gradient in the matrix is large. For smaller conductivity ratios, the fracture length with large pressure gradient reduces gradually (Fig. 4b and c). The extreme case is presented in Fig. 4a, where the low conductivity fracture reduces the length to near the wellbore vicinity. Fig. 5a–f shows the development of the pressure distribution in the matrix as a function of time, such that for long times, the profiles shown in Fig. 4a–d are attained. These figures correspond to the case when the fracture conductivity is moderately large. Initially, the pressure in the fracture is the same as that of the matrix, except in the limit of the reservoir, corresponding to zero pressure-gradient between fracture and matrix, or the condition of zero flow-rate. This condition allows starting from zero flow-rate up to that consistent with increasing pressure gradient. For non-dimensional times of the order of 0.05, the pressure gradient develops $(t = 0.5)$ to eventually attain the steady-state condition at long times. For decreasing fracture conductivity, the variation of the pressure gradient dp/dz in the x-direction becomes non-uniform, since it diminishes along the x-axis, inducing a reduction in the flow rate. A low fracture conductivity induces an increase in the difference between the pressure gradient dp/dz at $x=0$ and at $x=1$, and in the extreme case of very low fracture conductivity, there is a small region where the pressure gradient is large, implying a large reduction in the flow rate. Based on these profiles, it is illustrative to plot the development of pressure profiles in the matrix as a function of time (see Fig. 6). At short times,

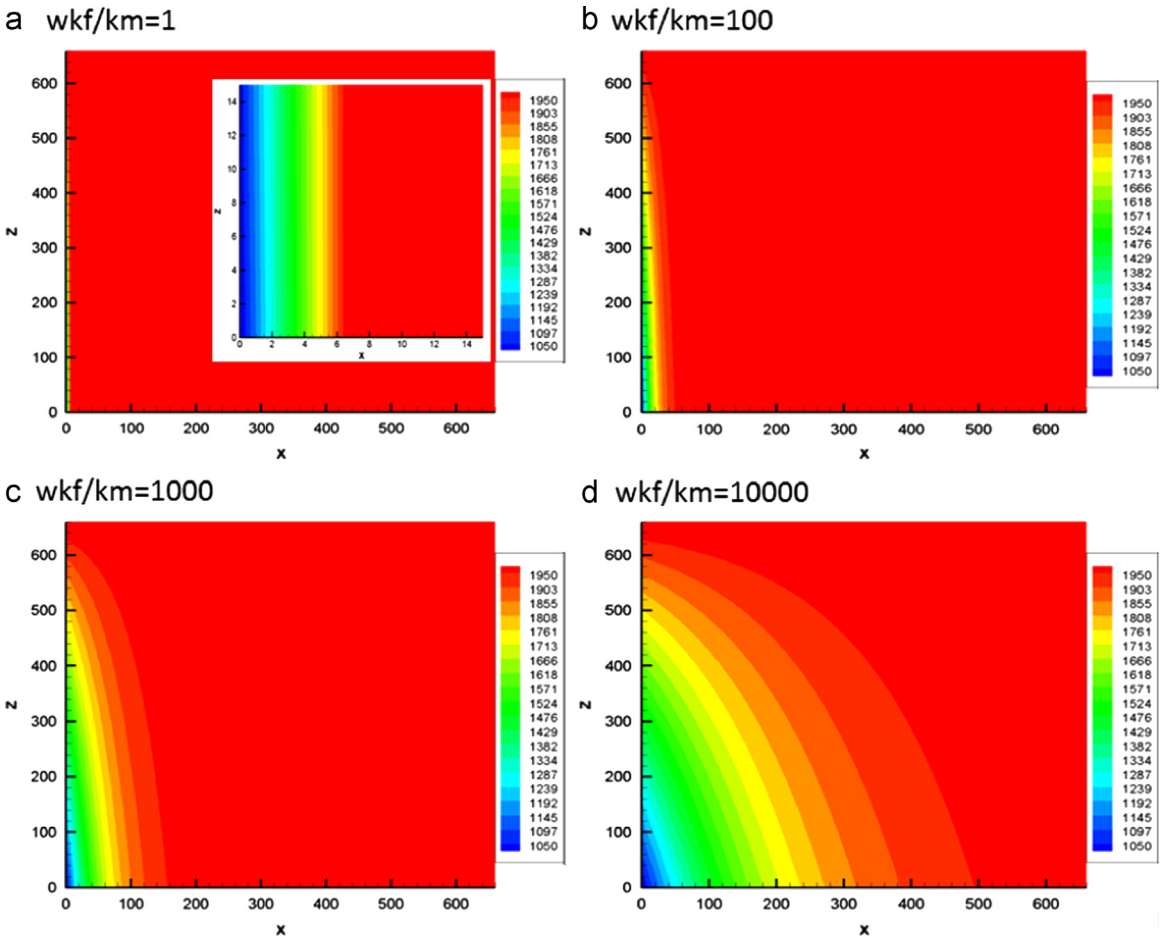

Fig. 4. Matrix pressure distribution under steady-state for various values of the non-dimensional fracture conductivity.

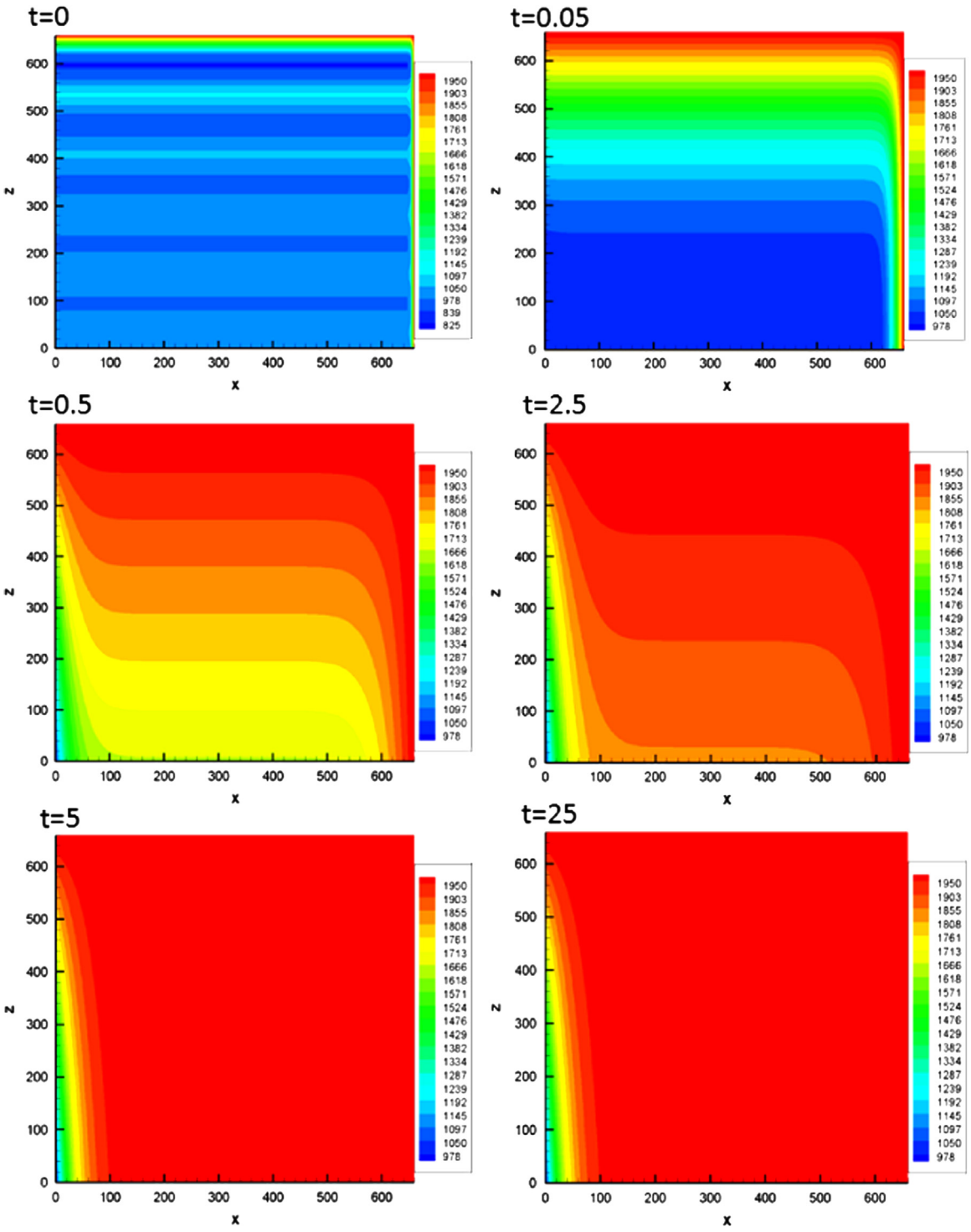

Fig. 5. Matrix pressure distribution for various dimensionless times. $Wk_f/k_m = 1000$ in.

the pressure gradient between the fracture and the matrix is near zero, this is, $p^* = 0$, except for $z^* = 1$, where $p^* = 1$. As time progresses, the pressure gradient develops up to a constant value, namely, steady-state at long times ($p^* = z^*$). Fig. 7 shows the development of the fracture pressure along the fracture length for several times, according to the solution of Eq. (25). The initial condition imposed is that, at $t=0$, the pressure in the matrix (p_m) is equal to the pressure along the fracture (p_f) which means zero pressure gradient or no-flow condition. The pressure profiles attain the steady-state pressure distribution for long times, given by Eq. (14). Indeed, as time increases, Eq. (25) reduces to Eq. (8), whose solution is Eq. (14). This is the case of where at long times, within a short length from the wellbore, the matrix pressure attains the value of the drainage pressure (see Fig. 5f, for $z=0$).

Fig. 8a describes the variation of the flow rate in the initial stage of the production and after the maximum flow rate, where it declines. The exponential increase and decrease is in accord to the solution given by Eqs. (30) and (37). At short times, both in the

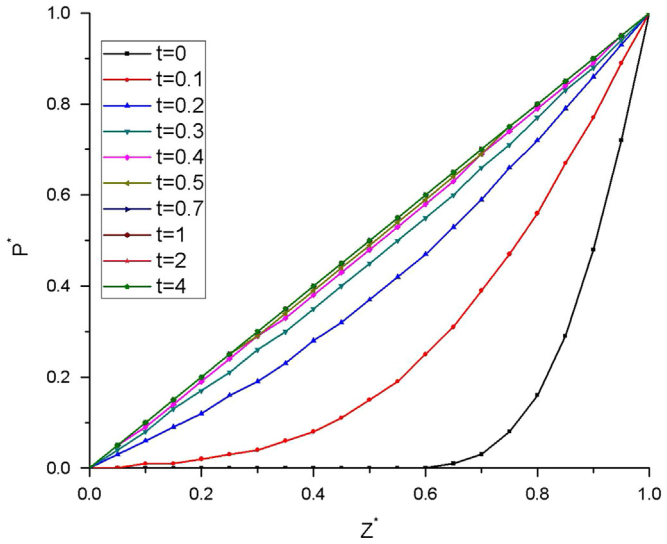

Fig. 6. Non-dimensional pressure as a function of non-dimensional distance along the matrix, for various dimensionless times. $Wk_f/k_m = 1000$ in.

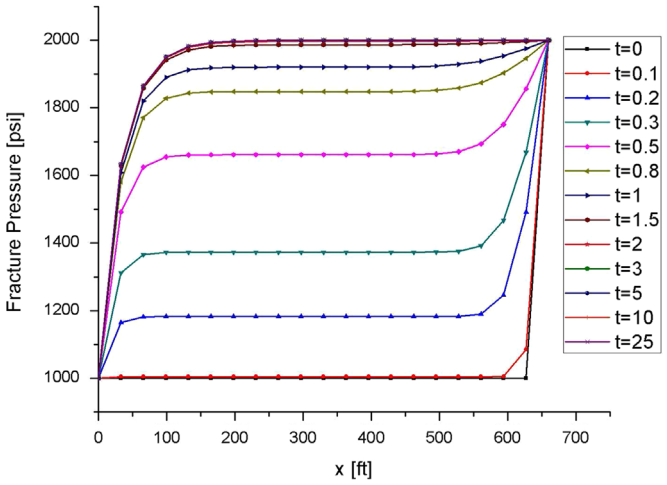

Fig. 7. Pressure along the fracture as a function of fracture length for various non-dimensional times. $Wk_f/k_m = 1000$ in.

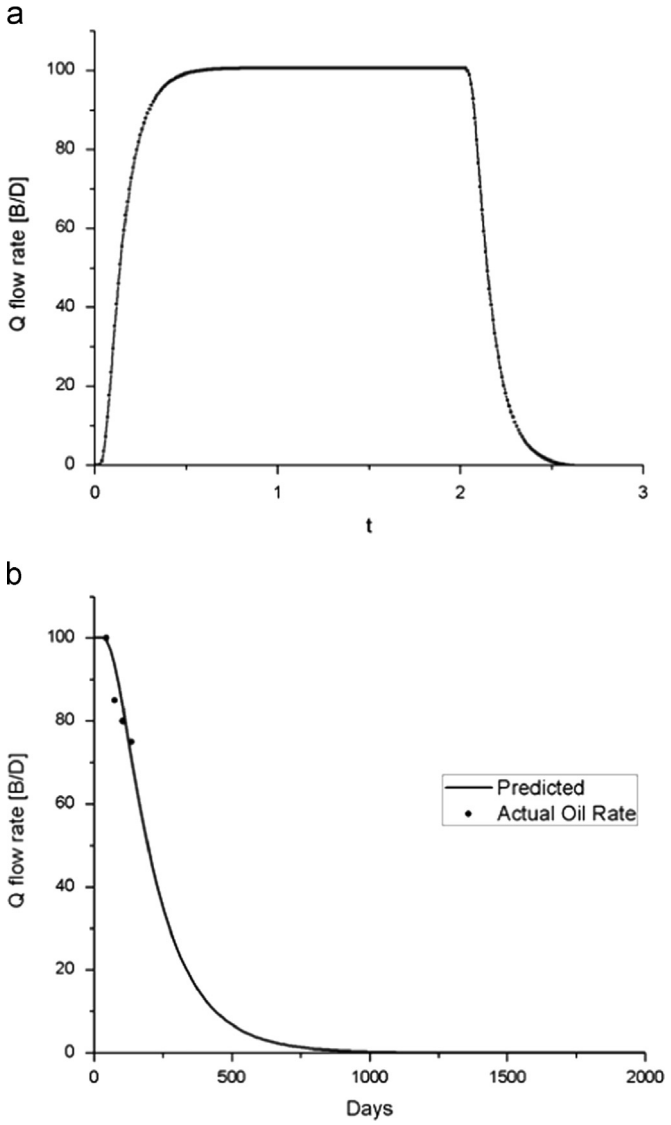

Fig. 8. Flow rate as a function of time. (a) Predictions of the production and declining stages. (b) Data from Table 1 (points) and predictions (continuous line).

increasing and decreasing modes, there is a linear relation of flow rate with time, which parallels the data shown in Table 1 for the decreasing mode. Data from Table 1 shows that the actual flow rate decreases linearly with time. Data points are indicated in Fig. 8b, and model predictions as a continuous line.

The Gringarten graphical type curve format is shown in Fig. 9. In this figure, the dimensionless pressure P_D versus the dimensionless ratio t_D/C_D is plotted. The resulting curves with varying C_D values represent different well conditions. All the curves merge, in early time, corresponding to pure-wellbore storage flow. During later times, at the end of the wellbore storage-dominated period, curves correspond to infinite-acting radial flow. Bourdet et al. (1983) proposed that flow regimes can have clear characteristic shapes if the pressure derivative rather than pressure is plotted versus time on the log–log coordinates. The use of this method for the entire well test will produce two straight lines that characterize the wellbore storage-dominated flow and the transient-flow period. Fig. 10 presents the pressure derivative versus t_D/C_D varying C_D. The early-time points are identified with straight lines with 45 angle slopes. Severe oscillations are neglected, since the radial infinite-acting state is not sufficiently clear.

Table 1
Data used for matching the production decline, as reported in Agarwal et al. (1970).

Month during 1952	March	April	May	June
Matrix permeability (md)	0.8	0.8	0.8	0.8
Water saturation	0.38	0.38	0.38	0.38
Residual oil saturation	0.15	0.15	0.15	0.15
Oil viscosity (cP)	0.90	0.95	1.0	1.0
Formation volume factor	1.310	1.295	1.285	1.285
Fracture spacing (ft)	3	3	3	3
Fracture length (ft)	600	600	600	600
Fracture height (ft)	15	15	15	15
Initial fracture width (in)	0.005	0.005	0.005	0.005
Initial fracture porosity	0.6	0.6	0.6	0.6
Number of fractures	5	5	5	5
Reservoir pressure (psig)	1650	1600	1500	1400
Bottom hole pressure (psig)	1000	1000	800	750
Stress sensitivity factor	0.1	0.1	0.1	0.1
Calculated oil rate (bopd)	101	89	84	75
Actual oil rate (bopd)	100	85	80	75

4. Conclusions

Cinco-Ley and Samaniego (1981) have presented a

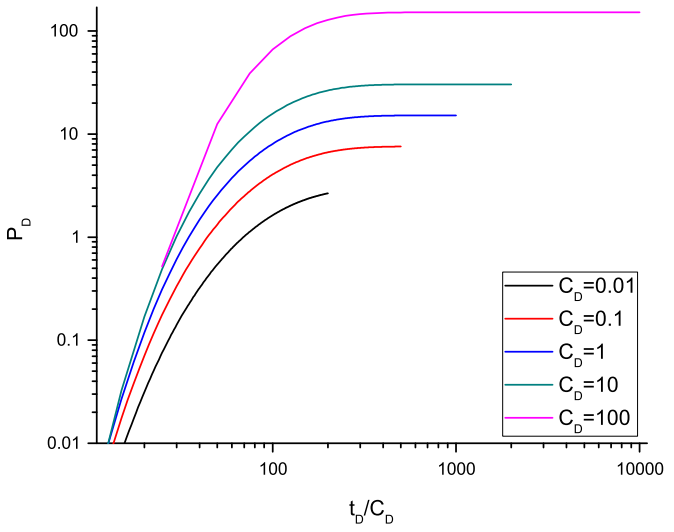

Fig. 9. Dimensionless pressure type curves for various dimensionless storage coefficient.

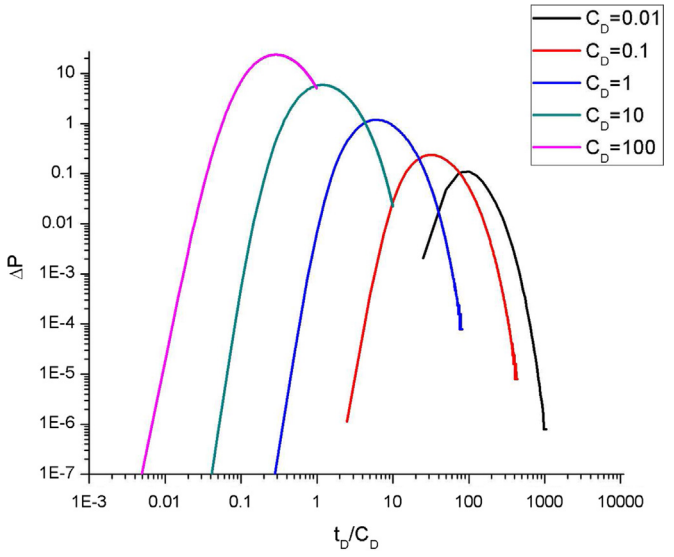

Fig. 10. Pressure derivative type curves for various dimensionless storage coefficient.

mathematical model by which, in a simple and concise form, steady-state predictions on the performance of vertical and horizontal wells intersecting fractures are exposed. The model allows a rigorous coupling of flows in the matrix and along the fracture, inasmuch as a unique pressure distribution in the fracture is used for both flows in the matrix and fracture. The model has been used in real situations where hydraulically fractured horizontal wells and vertical wells in naturally fractured reservoirs exist, generating the data shown in Table 1. Nonetheless, the transient decline of pressure and production rate cannot be calculated with this model. On the other hand, Cinco-Ley and Samaniego have developed techniques for analyzing pressure transient data for wells intercepted by a finite-conductivity vertical fracture, which is based on the bilinear flow theory, considering transient linear flow in both fracture and formation. We have shown here that the time-dependent generalization of the Guo et al. model is consistent with the Cinco-ley et al. model, and furthermore, that transient data of these complicated wells may be predicted.

Numerical simulations show that this simple and easy to implement model accurately reproduces previously reported data and can be used as a pressure-transient analysis or diagnostic tool to interpret complex characteristics and to investigate the influence of various fracture properties on the production performance of fractured horizontal wells.

Acknowledgments

The financial support of CONACyT, Mexico, through grants 116458 and 219810 is gratefully acknowledged. The authors thank Jose Manuel Reyes-Aguirre and Guillermo Gutierrez-Murillo of PEMEX E&P for fruitful discussions.

References

Agarwal, R.G., Al-Hussainy, R., Ramey Jr., H.J., 1970. An investigation of wellbore storage and skin effect in unsteady liquid flow: I. Analytical treatment. SPE J., 279–290.
Al-Kobaisi, M., Ozkan, E., 2004. A hybrid numerical analytical model of finite conductivity vertical fractures intercepted by a horizontal well. SPE 92040, pp. 1749–1766.
Al-Kobaisi, M., Ozkan, E., Kasogi, H., Ramirez, B., 2006. Pressure transient analysis of horizontal wells with transverse finite-conductivity fractures. Presented at the Petroleum Society's Seventh Canadian International Petroleum Conference (The 57th Annual Technical Meeting), Calgary, Alberta, Canada, 13–15 June, PETSOC 126.
Anh, V.D., Tiab, D., 2009. Transient pressure analysis of a well with an inclined hydraulic fracture using Tiab´s direct synthesis technique. Presented at the 2009 SPE Production Operations Symposium Held in Oklahoma City, OK, USA, April 4–8, SPE 120545.
Benjamin, J., 1978. Transient flow to finite conductivity fractures. SPE.
Biryukov, D., Kuchuk, F.J., 2012. Transient pressure behavior of reservoirs with discrete conductive faults and fractures. Transp. Porous Med. 95, 239–268.
Bourdet, D., Whittle, T.M., Douglas, A.A., Pirard, Y.M., 1983. A new set of type curves simplifies well test analysis. World Oil (May), 95–106.
Boussila, A.K., Tiab, D., 2003. Pressure behavior of well near a leaky boundary in heterogeneous reservoirs. SPE 80911, pp. 22–25.
Cinco-Ley, H., 1974. Unsteady-State Pressure Distribution Created by a Slanted Well or a Well with an Inclined Fracture (Ph.D. dissertation). Stanford University, California.
Cinco-Ley, H., Meng, Z., 1988. Pressure transient analysis of wells with finite conductivity vertical fractures in double porosity reservoirs. Presented at the 63rd Annual Technical Conference and Exhibition of the Society of Petroleum Engineers Held in Houston, TX, October 2–5, SPE 18172.
Cinco-Ley, H., Samaniego, F., 1981. Transient pressure analysis: finite conductivity fracture case versus damage fracture case. SPE 10179, pp. 1749–1766.
Gringarten, A.C., Bourdet, D.P., Landel, P.A., Kniazeff, V.J., 1970. Comparison between different skin and wellbore storage type-curves for early time transient analysis. In: SPE-8205, SPE-AIME 54th Annual Technical Conference, Las Vegas, Nevada, 23–25.
Gringarten, A.C., Ramey, H.J., 1973. The use of source and Greens function in solving unsteady-flow problem in reservoir. SPE J., 3818.
Guo, B., Schechter, D.S., 1997. A simple and rigorous mathematical model for estimating inflow performance of wells intersecting long fractures. SPE 38104, pp. 645–659.
Katz, A.J., Thompson, A.H., 1985. Fractal standstone pores: implications for conductivity and pore formation. Phys. Rev. Lett. 54, 1325–1328.
Kuchuk, F., Biryukov, D., 2012. Transient pressure test interpretation from continuously and discretely fractured reservoirs. Reserv. Eval. Eng. 17, 82–97, SPE-15096.
Ley, H.C., Samaniego, V.F., 1982. Pressure transient analysis for naturally fractured reservoirs. SPE 11026, pp. 26–29.
Makse, H.A., A. Jr., J.S., Stanley, H.E., 2000. Tracer dispersion in a percolation network with spatial correlations. Phys. Rev. E 61, 583–586.
Najurieta, H.L., 1980. A theory for pressure transient analysis in naturally fractured reservoir. J. Pet. Technol., 1241–1250.
Nelson, R.A., 1985. Geologic Analysis of Naturally Fractured Reservoirs.
Ozkan, E., 1988. Performance of Horizontal Wells (Ph.D. dissertation). The University of Tulsa.
Raghavan, R., Chin-Cheng, C., Bijin, A., 1997. An Analysis of horizontal wells intercepted by multiple fractures. SPE 27652.
Rbeawi, S.A., Tiab, D., 2012. Pressure behavior of partially penetrating multiple hydraulic fractures. Energy Environ. Res. 2 (1), 244–271.
Schmittbuhl, J., Steyer, A., Jouniaux, L., Toussaint, R., 2008. Fracture morphology and viscous transport. Int. J. Rock Mech. Min. Sci. 45, 422–430.
Song, B., Economides, M.J., Ehlig-Economides, C.A., 2011. Design of multiple transverse fracture horizontal wells in shale gas reservoirs. SPE 140555.
Streltsova, T.D., 1982. Well pressure behavior of a naturally fractured reservoir. Paper SPE 10782. pp. 769–780.
Turcio, M., Reyes, J.M., Camacho, R., Lira-Galenana, C., Vargas, R.O., Manero, O., 2013.

Calculation of effective permeability for the bmp model in fractal porous media. J. Pet. Sci. 103, 51–60.
Wan, J., Aziz, K., 1999. Multiple hydraulic fractures in horizontal wells. SPE 54627.
Warren, J.E., Root, P.J., 1963. The behavior of naturally fractured reservoirs. SPE J., 245–255.
Wong, D., Harrington, A., Cinco-Ley, H., 1986. Application of the pressure derivative function in the pressure transient testing of fractured wells. SPE 13056, pp. 470–480.
Zerzar, A., Bettam, Y., Tiab, D., 2003. Interpretation of multiple hydraulic fractured horizontal wells in closed systems. SPE 84888.